3D-Printing Nanocellulose-Poly(3-hydroxybutyrate- co -3-hydroxyhexanoate) Biodegradable Composites by Fused Deposition Modeling

3D Printing Nanocellulose-Poly(3-hydroxybutyrate-*co*-3-hydroxyhexanoate) Biodegradable Composites by Fused Deposition Modeling

Alberto Giubilini,[†] Gilberto Siqueira,[‡] Frank J. Clemens,[§] Corrado Sciancalepore,[†] Massimo Messori,[∥] Gustav Nyström,*[,‡,#] and Federica Bondioli*[,††]

[†] Department of Engineering and Architecture, University of Parma, Parco Area delle Scienze 181/A, Parma, 43124, Italy

[‡] Cellulose & Wood Materials Laboratory, Empa Swiss Federal Laboratories for Materials Science and Technology, Überlandstrasse 129, Dübendorf, 8600, Switzerland

[§] Laboratory for High Performance Ceramics, Empa Swiss Federal Laboratories for Materials Science and Technology, Überlandstrasse 129, Dübendorf, 8600, Switzerland

[∥] Department of Engineering "Enzo Ferrari", University of Modena and Reggio Emilia, Via Pietro Vivarelli 10, Modena, 41125, Italy

[#] Department of Health Sciences and Technology, ETH Zürich, Universitätstrasse 2, Zürich, 8092, Switzerland

[††] Department of Applied Science and Technology, Politecnico di Torino, Corso Duca degli Abruzzi 24, Torino, 10129, Italy

Corresponding Authors:
* E-mail: gustav.nystoem@empa.ch
* E-mail: federica.bondioli@polito.it

ABSTRACT: Fabrication of new bio-based composites with remarkable properties offers an attractive pathway for producing environmentally friendly materials. Here, a reinforcement for poly(3-hydroxybutyrate-*co*-3-hydroxyhexanoate) (PHBH) with functionalized cellulose nanocrystals (CNC) is presented and used to successfully 3D print such composites by fused deposition modeling (FDM). Acetylated CNC content varies from 5 to 20 wt%, in order to evaluate the effect of reinforcing agent on thermal and mechanical properties in the composites. The reinforcing effect of CNC is investigated by dynamic mechanical, thermal and rheological analysis. Thermogravimetric analysis and infrared spectroscopy allow to assert the success of chemical functionalization, whereas transmission electron microscopy is used to evaluate the impact of chemical modification on the morphology of the crystals. 3D printability of bio-based composites is proved by developing structures of complex designs with a FDM printer. Finally, the degree of disintegration under composting conditions is studied. Findings from these tests serve as an important step forward toward the development of eco-friendly materials for 3D printing complex architectures with tailored mechanical properties and functionalities.

KEYWORDS: poly(3-hydroxybutyrate-co-3-hydroxyhexanoate), cellulose nanocrystals, acetylation, melt compounding, fused deposition modeling, biodegradation

INTRODUCTION

Interest in bioplastics has exponentially increased in the last decades, due to the growing relevance of environmental issues as depletion of fossil resources and waste management. For this reason, nowadays, sustainability is playing a leading role in scientific research as well as technological and industrial implications. Polyhydroxyalkanoates (PHAs) are a new broad class of bio-based biodegradable aliphatic polyesters, which assumed great prominence in recent years owing, first of all, to their origin from renewable resources and their sustainable end-of-life. Moreover, in accordance with the constituent monomers they possess, PHAs can vary within a wide spectrum of properties, concerning for example degree of crystallinity, melting temperature or stiffness. Among these biopolymers, poly(3-hydroxybutyrate-*co*-3-hydroxyhexanoate) (PHBH) is a thermoplastic copolymer synthesized by bacteria and other microorgan-

isms under imbalanced conditions of nitrogen and oxygen.[1] It consists of two different monomers: 3-hydroxybutyrate (3HB) and 3-hydroxyhexanoate (3HH), and their molar ratio influences the properties of the copolymer.[2]

The fabrication of environment-friendly reinforced plastics holds a huge potential since they combine sustainability and competitive properties (i.e. stiffness and strength, thermal stability and/or gas barrier functionality) in a single material. Previous research has focused on different reinforcing effects of some agents, such as glass fibers[3] for improving the stiffness and the strength, or graphene oxide[4] for increasing the gas barrier properties and for decreasing the diffusivity. Particular interest has been reserved for natural reinforcements, as nanocellulose[5,6] for increasing the toughness and the tensile strength of the composite, due to its biodegradability, biocompatibility, and outstanding mechanical properties,[7,8] or also to industrial by-product of plant origin,[9] used as filler, to reduce the cost of the final material.

Concerning its origin and morphological structure, nanocellulose may be differentiated into bacterial cellulose (BC), cellulose nanofibrils (CNF) and cellulose nanocrystals (CNC). CNC are obtained by acid hydrolysis, they have a crystalline structure and they are needle-shaped with 150-300 nm in length and 5-10 nm in diameter.[10] Mechanical treatment, such as homogenization or grinding, can transform cellulose fibers into CNF. These last have a web-like structure with a diameter of 5-60 nm and a length of several micrometers.[8] Along these fibrils, crystalline regions and amorphous regions alternate. The impressive mechanical reinforcement effect of these materials is not only due to their high aspect ratio but also to the stiffness of these nanocomponents: Young modulus was calculated to be about 140 GPa for CNC[11] and 100 GPa for CNF.[8] In this work the reinforcing effect of CNC on PHBH properties was investigated. Previous research indicates that a great challenge when compounding nanocellulose and biopolymers is avoiding nanoparticle aggregations and obtaining a good adhesion between the hydrophobic matrix and the hydrophilic filler.[12,13] Different approaches have been experimented for functionalization of nanocelluloses as: esterification,[14,15] acetylation,[16,17] silanization,[18,19] TEMPO_mediated oxidation,[20,21] amidation[22] and polymer grafting.[23,24] All of them have the same purposes, namely to enhance the affinity with the polymeric matrix or to enable their dispersion in organic solvents. Here, we carried out an acetylation process, aimed to bond acetyl groups (-CO-CH_3) onto cellulose surface. We followed this functionalization due to the expected chemical affinity between the C=O group of PHBH and the -CO-CH_3 group of acetylated CNC.

To date, cellulose-based nanocomposites have been explored in different matrices and at different reinforcing content.[25–27] However, the majority of the work related to the compounding of nanocellulose and thermoplastic polymers are processed by solution casting, a method that requires a high amount of organic solvents such as chloroform or dimethylformamide,[5,28] inhibiting the application to industrial level, and highly limiting the possible final shapes of the objects. Here, we utilized a melt compounding process, preceded by a solvent premixing step, to obtain the final bio-based composites. This procedure combined the advantages of melt compounding with the ones of solvent pre-mixing thus avoiding CNC aggregation during the drying process and obtaining a good dispersion of CNC in PHBH compared to direct melt compounding of the biopolymer pellets with the dry powder of acetylated CNC. Therefore, we considerably reduced the amount of environmentally harmful and toxic solvents and we suggested a process that could be more easily scaled up for industrial applications. Moreover, we did not limit the research to the fabrication of new bio-based composites, but we pushed the investigation towards a possible application in a field of increasing interest: additive manufacturing.

Fused deposition modeling (FDM) is an extrusion-based 3D printing technique that enables the construction of 3D structures allowing different thermoplastic polymers to be printed at the microscale.[29,30] Some materials have been studied more extensively so far, and they are commonly used, such as poly(acrylonitrile-*co*-butadiene-*co*-styrene) (ABS),[31,32] poly(lactic acid) (PLA)[33,34] or polycaprolactone (PCL).[35,36] Nowadays, the new challenging frontier of FDM is the use of unconventional polymers with original properties and different possible applications. To the knowledge of the authors, previous research investigating PHBH 3D printability is still extremely limited, and there is only one research focused on FDM 3D printing of PHBH and CNF.[37] Furthermore, the findings obtained in this study are referred to composites with low CNF content (up to 3 wt%) and the mechanical properties obtained are inferior to pristine PHBH, probably due to a low affinity between matrix and CNF. Here, we developed bio-based composites at high CNC content (5-20 wt%), which were first acetylated to improve the interaction of the nanocellulose and the matrix and thus to obtain an enhancement in mechanical and thermal properties of the final composite. Subsequently, we 3D printed this innovative material to realize

complex and fully biodegradable architectures. In this way, we managed to mix the advantages of eco-friendly material with the production of objects with customizable designs by additive manufacturing.

EXPERIMENTAL SECTION

Materials: Poly(3-hydroxybutirate-*co*-3-hydroxyhexanoate) (PHBH) containing 11 mol% of hydroxyhexanoate was supplied by MAIP Group in pellet form. Cellulose NanoCrystals (CNCs) were purchased from CelluForce. According to the elaboration of the TEM images, nanocrystals have an average length (L) of 120 nm and an average diameter (d) of 6.5 nm and they possess an aspect ratio of about 18. Low-density polyethylene (LDPE) pellets were used as a comparison for disintegration with biopolymers, and they were purchased from Versalis S.p.A. Chloroform was purchased from VWR, acetic anhydride and sulfuric acid (95-97 %) were purchased from Merck. Before any processing, PHBH pellets were oven-dried at 85 °C overnight.

Chemical modification of CNC: The acetylation process was run following a precedent research of Olaru *et al.*[38] without use of any solvent. First, acetic anhydride (75 mL) was mixed with sulfuric acid (150 µL), used as a catalyst, and then CNC (15 g) was added to this solution under mechanical stirring at 250 rpm. Acetylation reaction was performed in a round-bottom flask immersed in an oil bath at 30 °C for different reaction times: 1, 2, 8 or 20 hours. When the desired reaction time expired, each sample was washed four times using a centrifuge at 5000 rpm for 10 minutes. The precipitated modified CNCs were subsequently redispersed and solvent exchanged first with ethanol, then with acetone and finally with chloroform. All centrifugation operations were conducted at 5000 rpm for 10 minutes. Each redispersion step was carried out using an Ultra-Turrax T25 mixer. Samples were never dried, except for the samples used for FT-IR analysis, which were air-dried for 24 hours and then dried for 8 hours in oven at 45 °C.

Filament preparation for FDM printing: Acetylated CNC was added by solution mixing to the PHBH in order to obtain masterbatches of PHBH matrix, filled with modified cellulose nanocrystals. PHBH pellets were added to chloroform and stirred until complete dissolution and the acetylated CNC dispersed in chloroform were added and let stirring for further 4 hours at room temperature. The obtained dispersion was subsequently poured into a Petri dish. The drying process was performed, first, overnight at room temperature and finished in oven at 45 °C for 5 hours. The obtained films were used like masterbatches, and so they were cut into smaller pieces and used for further compounding with neat PHBH pellets in order to obtain composites at different filler content: 5 wt%, 10 wt%, 15 wt% and 20 wt%. The second compounding was obtained using high shear mixing Rheomix 300 (PolyLab OS, Thermo Electron Corporation, Germany) with roller rotors at a processing temperature of 145 °C, a mixing speed of 10 rpm and a mixing time of 20 min. The obtained compounded materials filled in a capillary rheometer (Rosand RH7, Netzsch GmbH, Germany) and filaments with a diameter of 1.75 ± 0.05 mm were obtained using a capillary die with an orifice of 1.8 mm, a temperature of 145 °C, and an extrusion speed of 8.5 mm min^{-1}.

3D printed samples by FDM: A K8200 3D printer (Velleman NV, Belgien) was fed with the extruded filaments of neat biopolymer and all composites. The bed temperature of the printer was 50 °C, the nozzle temperature 170 °C, the printing speed 5 mm s^{-1}, and a linear infill type was used with a fill percentage of 100 %. Nozzles of 0.6 mm and 0.4 mm were used to print layer heights of 0.48 mm and 0.32 mm, respectively.

In order to evaluate the shear rate experienced by the filament during the FDM printing, it was associated to that of a capillary system,[39] and therefore, we can express shear rate as:

$$\dot{\gamma} = \frac{4Q}{\pi r^3} \quad (1)$$

where Q is the flow rate and r is the radius of the nozzle of the printer. Moreover, considering the flow rate as:

$$Q = \pi r^2 v \quad (2)$$

where v is the printing speed; and combining the two previously equations, we can express the shear rate as a function of printing speed and nozzle radius; and precisely we can affirm that:

$$\dot{\gamma} = \frac{4v}{r} \quad (3)$$

Assuming a printing speed of 5 mm s^{-1} and a nozzle diameter of 0.4 mm, we obtain a typical shear rate of 100 s^{-1} experienced by the melt polymer during the extrusion through the nozzle.

Transmission Electron Microscopy (TEM): Morphology of used CNC was evaluated by Transmission Electron Microscopy (Jeol JEM-2200FS, USA Inc.) using an acceleration voltage of 200 kV. Plasma-activated carbon-coated grids were used as support onto which both 0.01 wt/v% diluted suspensions of CNC in water were deposited, before and after the functionalization. The average diameter and length of

CNC were measured using the measuring tool in ImageJ software.

Environmental Scanning Electron Microscopy (ESEM): In order to obtain information on the variation of the polymeric microstructure over time as a result of the fragmentation process, sample microscopies were acquired by means of the environmental scanning electron microscope ESEM Quanta-200 (Fei Company, USA). The samples were analyzed in low vacuum conditions, using the solid-state detector for the backscattered electron imaging signal collection. The accelerating voltage of 15kV, the spot size of 5 and the working distance of 11mm were used in the acquisition of all images.

Fourier Transform Infrared Spectroscopy (FT-IR): Infrared spectra of dried unmodified and acetylated CNC (i.e., air-dried for 24 hours and then dried for 8 hours in oven at 45 °C) were recorded on a Tensor 27 FT-IR spectrometer (Bruker Corporation, USA) in attenuated total reflectance mode. The spectra were recorded between 4000 and 500 cm^{-1}, with a resolution of 4 cm^{-1} and 32 scans. The chemical acetylation of CNC over time was evaluated calculating the absorption ratio (A_r):

$$A_r = \frac{I_{1745}}{I_{1160}} \quad (4)$$

where I_{1745} is the intensity of the C=O stretching band at 1745 cm^{-1}, used to quantify the grafted acetyl group onto cellulose structure,[40] and I_{1160} is the intensity of the antisymmetric bridge oxygen stretching band of the cellulose molecular skeleton, used to characterize cellulose, since it does not change during acetylation.[41] A_r can be considered a suitable qualitative indicator of the acetylation process over time since it is proportional to the degree of acetylation (DS) according to this relation:

$$A_r = \varepsilon \cdot \mathrm{DS} \quad (5)$$

where ε is a constant, defined as the absorptivity ratios of the bands at 1745 cm^{-1} and 1160 cm^{-1}.[41]

Rheological Analysis: Rheological properties of pristine PHBH and related composites were determined using a rotational rheometer Anton Paar MCR 502 with a 15 mm parallel plate geometry, a gap of 0.5 mm at constant temperature of 170 °C. Flow curves under shear rates ranging from 10^{-3} to 10 s^{-1} were obtained through time-controlled measurements. Above 10 s^{-1} the sample was leaving the gap.

Thermogravimetric Analysis (TGA): Thermogravimetric Analysis were conducted on a STA 449 F3 Jupiter (Netzsch GmbH, Germany). Each sample was heated from 50 to 600 °C at a ramp of 5 °C min^{-1} in air.

Dynamic Mechanical Analysis (DMA): Dynamic Mechanical Analysis was performed with a three-point bending clamp, in temperature ramp/frequency sweep mode using an RSA III from TA Instruments (Delaware, USA) with heating rate of 3 °C min^{-1}. All samples were 3D printed with dimensions 45 x 5 x 1.5 mm^3 (length x width x thickness) and were scanned over a temperature range from -50 to 110 °C, applying a strain of 0.1 %, under the frequency of 1 Hz. All samples were equilibrated for 10 minutes at -50 °C before starting the analysis, in order to homogenize the temperature in the measuring chamber.

Disintegration under composting conditions: The disintegration of neat PHBH, PHBH bio-composites and LDPE was investigated under simulated composting conditions in a laboratory-scale test, as described in EN ISO 20200 standard. Solid synthetic waste was prepared by mixing 40 wt% sawdust supplied by sawmill Maletti Alfredo e figli S.r.l. (Modena, Italy), 30 wt% of rabbit food purchased from Valman S.r.l. (Vicenza, Italy), 10 wt% of ripe compost supplied by COMPO GmbH & Co. (Münster, Germany), 10 wt% of corn starch, 5 wt% of sugar, 4 wt% of corn seed oi and 1 wt% of urea. After mixing, distilled water was added to the obtained synthetic solid waste to adjust its final water content to 55 wt%. Water was then added periodically by adjusting the weight of the containers according to the procedure described in EN ISO 20200 standards, in order to maintain a sufficient and constant relative humidity in the compost medium. LDPE, PHBH and PHBH+CNC_AC composites were hot pressed at 120 °C for thirty seconds to produce squared films (25 x 25 x 0.5 mm^3). Each film was weighed and then buried in composting reactors at 5 cm depth, inside iron mesh bags to simplify their extraction and allow the contact of the compost with the specimens. The aerobic conditions were guaranteed by mixing the synthetic waste periodically, adding water according to the standard requirements and making a hole of 5 mm diameter on the side of the composting reactors, providing gas exchange between the inner atmosphere and the outside environment. Three replicates of each sample were buried and analyzed. Containers were incubated at 58 °C for 90 days in oven (ISCO NSV 9090 model). Films were recovered from the containers every week, washed with distilled water, dried overnight at 85 °C and reweighed. The degree of disintegration (D) of the samples was calculated by normalizing the sample weight, at different composting times, to the initial weight using this equation:

$$D = \frac{m_i - m_f}{m_i} \cdot 100 \quad (6)$$

where, m_i is the initial dry mass of the test material and m_f is the dry mass of the test material recovered at different incubation stages.

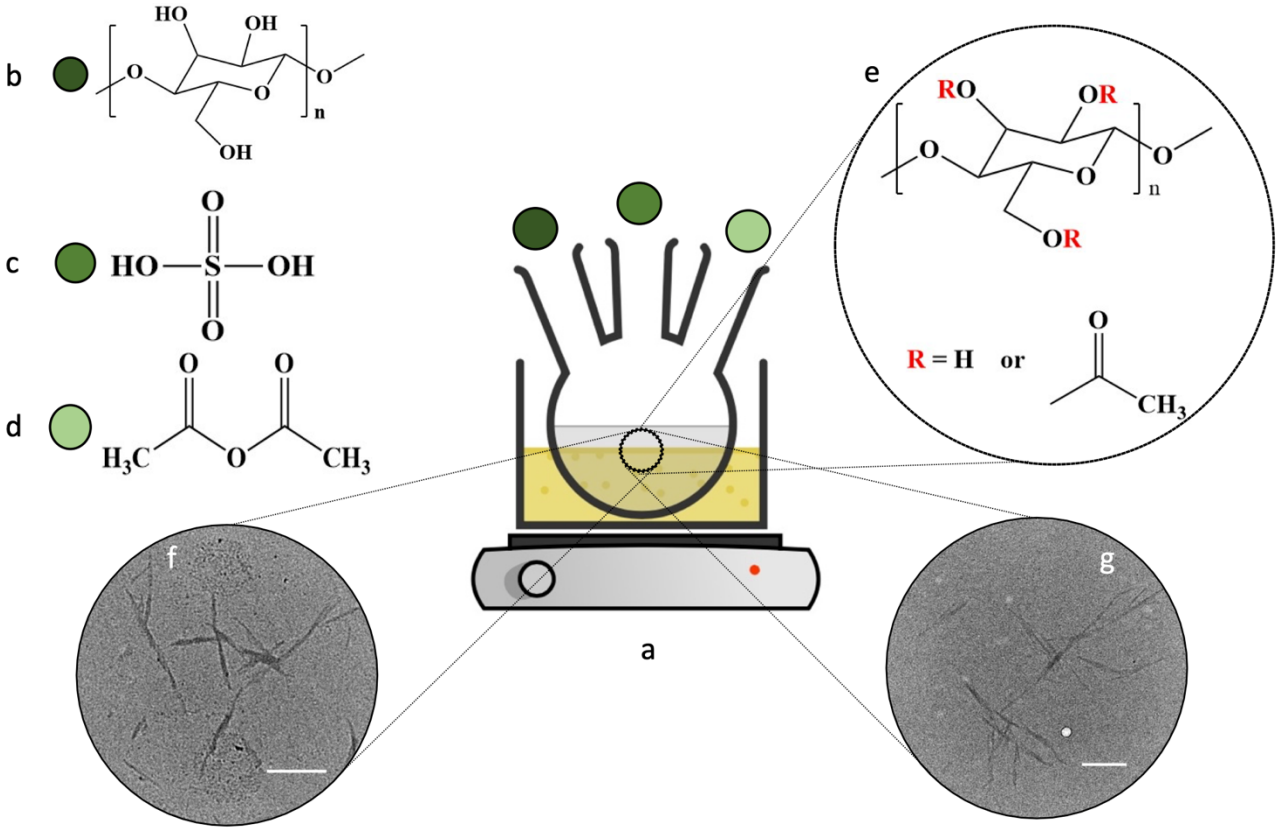

Figure 1. Schematic of the acetylation process of CNC particles (a), of the chemical structures of reagents: cellulose (b); sulfuric acid (c) and acetic anhydride (d) and of the acetylated cellulose after the functionalization (e), with the representation of acetyl groups bonded to the cellulose structure, replacing the hydroxyl groups. TEM images show unmodified CNC (f) and acetylated CNC after 8 hours of acetylation (g), scale bars 150 nm.

RESULTS AND DISCUSSION

To enhance the affinity and the compatibility between the hydrophilic reinforcing agent and the hydrophobic biopolymer matrix, we performed a surface modification of CNC. With this reaction, a desired surface functionality was introduced, which directly influences compatibility and dispersibility of CNC in the polymer matrix to achieve more homogenous composite microstructures. As discussed in the introduction, different functional groups have already been introduced to nanocelluloses by diversified processing routes.[14-24] Here, we decided to carry out an acetylation process, as shown in **Figure 1**, which aims to replace part of hydroxyl groups (-OH) of cellulose with acetyl groups (-CO-CH3). We focused on this kind of functionalization due to the chemical affinity between the C=O group of PHBH and the -CO-CH3 group of acetylated CNC, where strong dipole–dipole interactions are expected to be established.[42] Furthermore, we favored this particular acetylation procedure since it is a greener chemical route for grafting acetyl groups on CNC surface, as compared to the majority of processes, which employ organic solvent, like dimethylformamide (DMF) or pyridine, which have been extensively used in previous research,[40,43] and whose ecological impact is certainly negative.

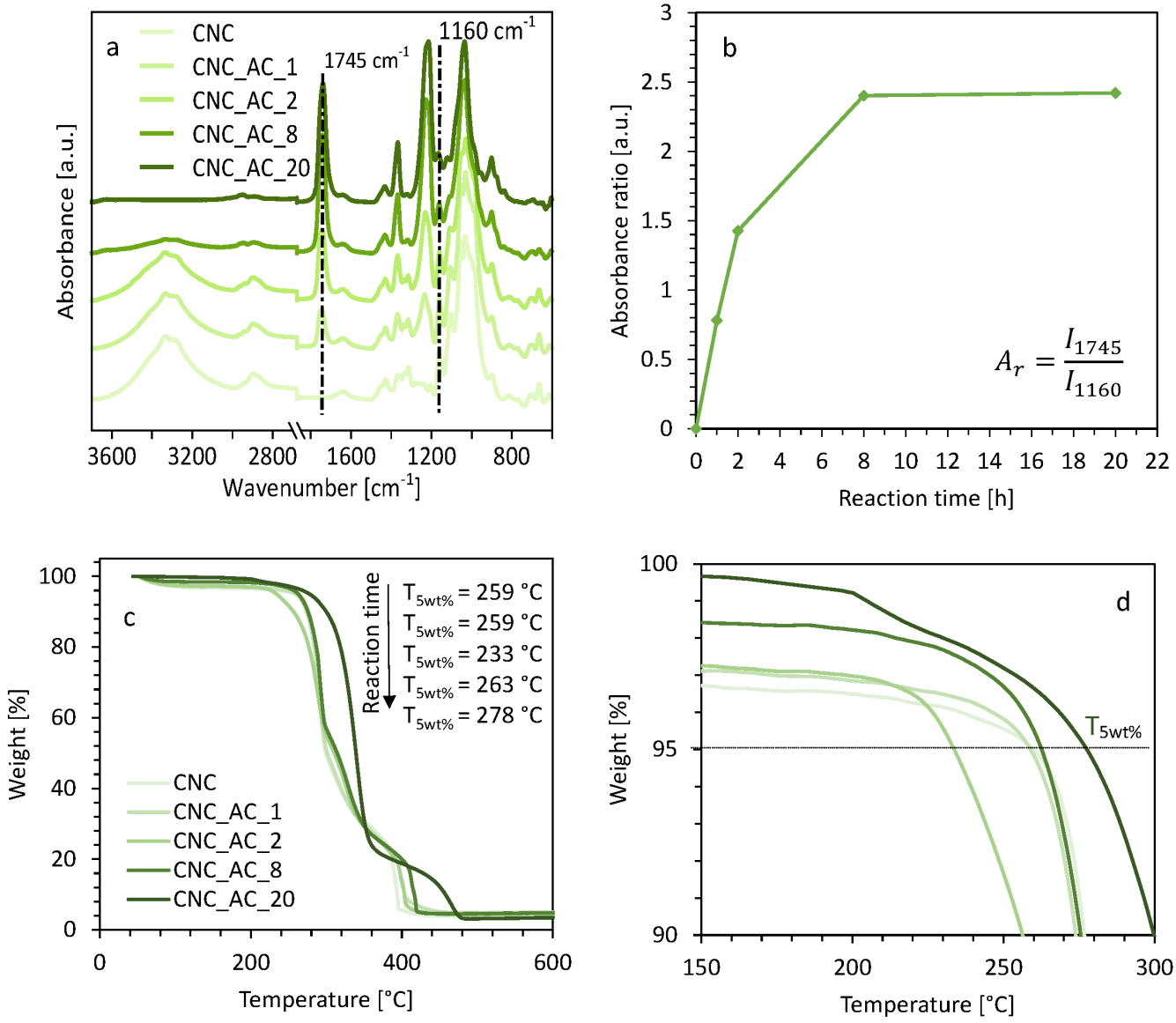

Figure 2. Chemical characterization by FT-IR analysis of the CNCs (a) and the absorbance ratio dependence over reaction time, as an indication of the degree of acetylation (b). Thermogravimetric analysis of pristine CNC and acetylated CNC at different reaction times (CNC_AC_X), where X corresponds to the reaction times expressed in hours (c). Zoom-in of the diagram for the evaluation of the effect of the acetylation process on the thermal stability of the powders, evaluated at 5 wt% of mass loss (d).

Clear indication that the functionalization occurred positively was given by the results of FT-IR characterization (**Figure 2** a). In all spectra three new characteristic peaks of acetyl group vibration at 1745 cm^{-1} [carbonyl stretching C=O], 1370 cm^{-1} [methyl in-plane bending in -O(C=O)-CH_3] and 1230 cm^{-1} [C-O stretching of acetyl group] are evident.[38,40,43,44] Moreover, it is evident the decrease of intensity of the broad band, with a maximum around 3340 cm^{-1}, typical of stretching of -OH groups, accordingly with a partial substitution of hydroxyl groups with acetyl groups.[44]

The functionalization was let to continue for different reaction times, in order to parametrically evaluate the chemical modification of CNC over time and the relative kinetics of the reaction. It can be seen from the FT-IR spectra that the reaction time increase correlates directly with the intensity of the new peaks (**Figure 2** b) and inversely with the broad band of hydroxyl group decrease.

For the development of this work, only CNC acetylated for 8 hours (CNC_AC_8) were taken in consideration, since they showed a good balance between a sufficiently high degree of acetylation without compromising neither the nanostructure nor the morphology of the nanocrystals, as proved by TEM images (**Figure 1** f and g). The accurate control of the acetylation degree is a relevant variable for the production of nanocomposites with specific properties. It has been proved that for longer acetylation times, and thereby

for higher degree of acetylation, significant changes in the cellulose crystalline structure can be promoted and, therefore, also variations of macroscopic properties, such as a decrease in crystallinity degree and an increase in thermal stability and degree of dispersion in organic solvents.[40] In this work, the substitution of hydroxyl groups with acetyl groups has an improving effect on the thermal stability of modified nanocrystals.[6] This was investigated by TGA and 5 % weight loss temperature ($T_{5wt\%}$) was chosen as a reference for thermal stability (**Figure 2** c and d). All curves show an initial decrease of weight due to the loss of moisture, but this is more evident in CNC, because of the higher amount of free hydroxyl groups compared to the acetylated samples.[45] At 5 % weight loss, a $T_{5wt\%}$ of 259 °C was measured for CNC, and this value shifts to higher values, except for the case with two hours of acetylation, where it decreases at 233 °C. The maximum $T_{5wt\%}$ is reached for twenty hours of acetylation and it corresponds to 278 °C. These results are useful to fully understand the effect of acetylated CNC on the thermal behavior of the final PHBH+CNC_AC_8 composites.

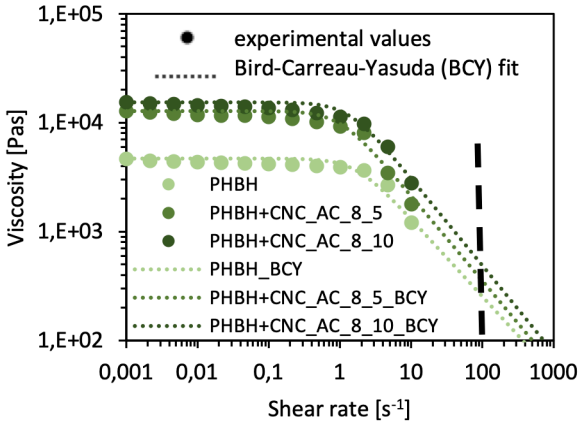

Figure 3. Rheological properties of compounded materials with different acetylated CNC content (CNC_AC_8_XX), where XX represents the reinforcing agent content expressed as weight percent (5 wt% and 10 wt%). Shear viscosity curves of neat PHBH and PHBH+CNC_AC_8 composites at different CNC content are plotted. The fit of the viscosity curves was obtained using the Bird-Carreau-Yasuda (BCY) model.

To estimate flow behavior of the nanocellulose-based compounds and to characterize their behavior during the printing process, we carried out rheological measurements. **Figure 3** presents 5 and 10 wt% acetylated CNC content; 15 and 20 wt% acetylated CNC content are shown in **Figure S1** (Supporting information).

All data were collected with a parallel plate rheometer with a shear rate up to 10 s^{-1}. To estimate the viscosity also for higher shear rate, these data were successively implemented with the empirical Bird-Carreau-Yasuda model:[46]

$$\eta = \eta_\infty + (\eta_0 - \eta_\infty)[1 + (\lambda\dot{\gamma})^2]^{\frac{n-1}{2}} \quad (7)$$

where η_0 represents the zero-shear rate viscosity, η_∞ represents the infinite shear rate viscosity and it can be assumed to be 0, λ is the relaxation time that reflects the onset shear rate of shear thinning and n is the power law index that affects the slope of the shear thinning region. The model parameters were determined starting from experimental data (**Table S1**, Supporting Information).

For shear rate below 1 s^{-1}, a plateau can be observed for all curves. As expected, by increasing the CNC content, the viscosity increases, due to the interactions between nanocrystals and matrix and between nanocrystals themselves that refrain chain movements and they hinder chain relaxation.[47] For shear rate above 1 s^{-1}, shear thinning behavior can be observed in all samples. However, the effect of the CNC content can be determined by the change of the exponent n of the Bird Carreau-Yasuda model. A lower exponent n result in a higher shear thinning effect of the material. Therefore, the increase of viscosity associated with the filling content is reduced and hence the differences between curves obtained at different CNC content are smaller.

Estimating at the typical shear rate for our FDM 3D printing process (100 s^{-1}), the viscosities vary from 250 Pas to around 500 Pas; and precisely, the obtained values are: 253 Pas for neat PHBH, 353 Pas, 487 Pas, 250 Pas and 266 Pas for 5 wt%, 10 wt%, 15 wt% and 20 wt% of acetylated CNC content, respectively. Measurements performed during the experiments allow to say that all compounds are printable, since all obtained viscosity values are within acceptable range of FDM 3D printability.[48,49]

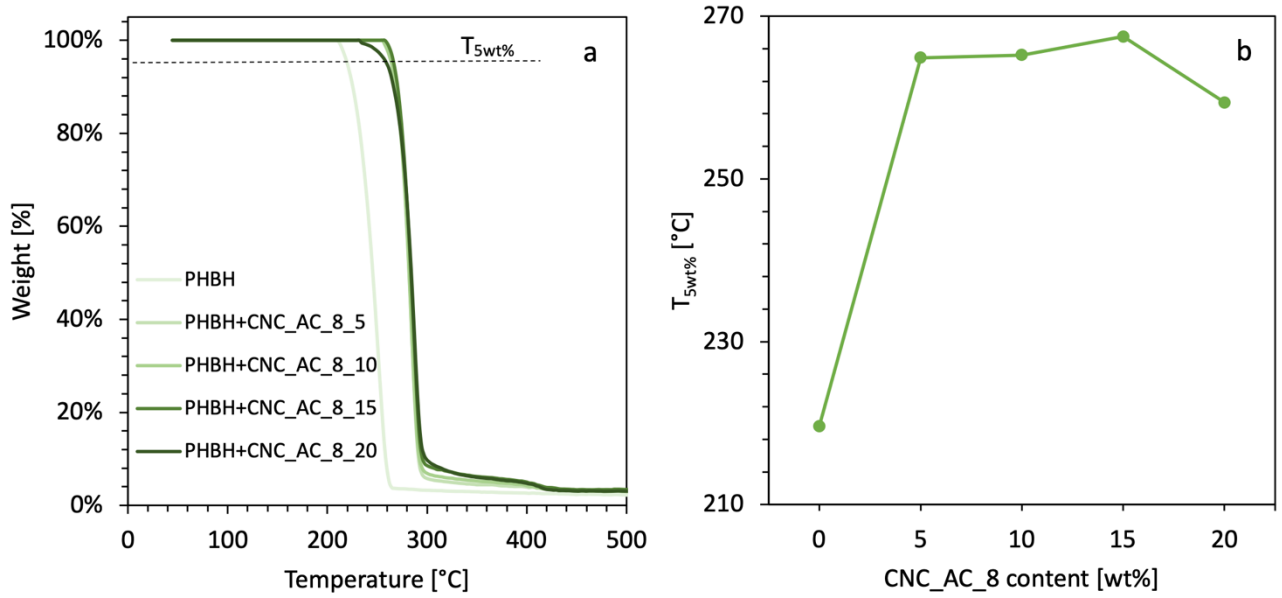

Figure 4. Thermal properties of PHBH and PHBH+CNC_AC_8 composites as a function of CNC content: 5 wt%, 10 wt%, 15 wt% and 20 wt%. Thermogravimetric analysis in air atmosphere (a). Thermal stability of composites evaluated at the temperature of 5 % of mass loss ($T_{5wt\%}$), which increases with the compounding of acetylated CNC, independently from its content (b).

To experimentally investigate the effect of the acetylated CNC on the thermal properties of the nanocellulose-based composites, we tested all compounded materials with TGA. **Figure 4** highlights the main results.

When evaluating this property at the temperature associated with a mass loss of 5 wt% ($T_{5wt\%}$), the effect of CNC addition on the thermal stability of neat PHBH is clearly observed. The thermal stability with respect to neat polymer is systematically shifted toward higher temperature, with an increase in thermal stability of about 45 °C, regardless of the filler content (see the Supporting Information). Starting from a temperature of 220 °C for neat PHBH, we reached an average value of 265 °C for CNC_AC_8 based composites. This property permits to widen the range of use of PHBH, considering also applications with higher working temperature conditions. The thermogravimetric measurements demonstrate that acetylated CNC improve the thermal stability of the neat PHBH matrix. The same trend has already been individuated in previous research,[6] however here we reached a fourfold improvement compared to the cited study.

To understand the enhancing effect of nanocellulose on the thermal properties of the PHBH matrix, it is important to consider the thermal degradation process of this polymer. Previous research indicates that this happens by a random chain scission reaction with a six-membered ring ester intermediate, transforming eventually the ester groups into olefinic and carboxylic acid groups.[50,51] The chain scission rate increases according to the increase in temperature, and therefore, at higher operating temperatures this degradation is faster. The formation of six-membered ring ester during the early stage of the PHBH degradation process is hindered by the intermolecular hydrogen bonding interactions that occur between the oxygen of the ester groups of the PHBH matrix and the unreacted hydroxyl groups of acetylated CNC or the acetyl group bonded to the CNC surface.[52]

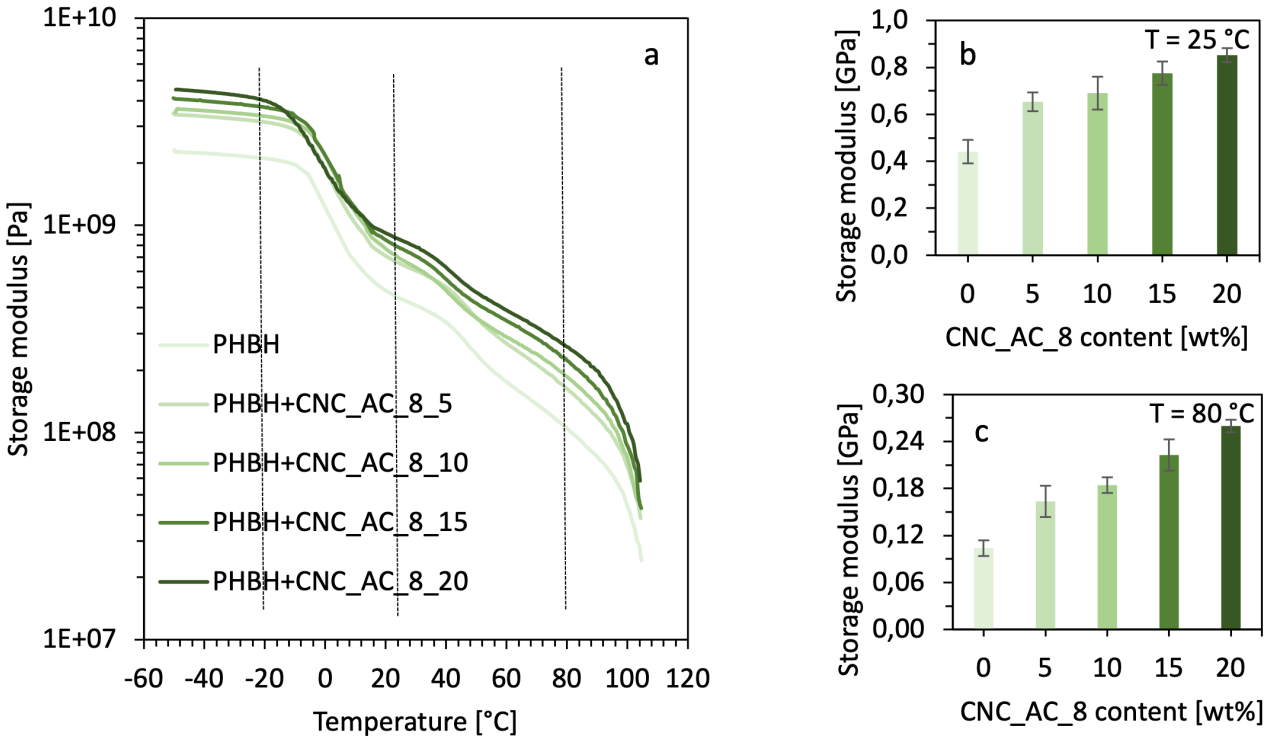

Figure 5. Thermal behavior of the storage modulus evaluated at different CNC contents: 5 wt%, 10 wt%, 15 wt% and 20 wt% (a). Storage modulus values as a function of CNC content evaluated at two particular temperature conditions: at room temperature T = 25 °C (b) and at high temperature, T = 80 °C (c). Error bars show the standard deviation for three measurements.

The results of Dynamic Mechanical Analysis (DMA) show the impact of acetylated cellulose nanocrystals on the storage modulus of PHBH matrix over all range of temperature. **Figure 5** highlights the main results (**Figure S3**, Supporting Information). The increase of storage modulus follows a typical trend observed for several cellulose-based composites being directly proportional to the addition of acetylated CNC and therefore the most noticeable reinforcing effect is observed for composites 20 wt% of acetylated CNC. The increase in the storage modulus is more or less constant both before and after the glass transition, indicating the transition from a brittle into a rubbery state. Three temperature conditions were considered for comparison: -20 °C as an indication for the glassy behavior, 25 °C as an indication for the room temperature behavior and 80 °C as an indication for a high temperature application of this material. The maximum relative increments of storage modulus, assuming the neat PHBH as the reference, were obtained at 80 °C, and they correspond to: 58 %, 78 %, 115 % and 150 % for 5, 10, 15 and 20 wt% acetylated CNC content, respectively (**Table S3**, Supporting Information). Moreover, it is important to note that, for the same value of storage modulus, acetylated CNC widens the range of temperatures of applications by a value of approximately 20 °C. This mechanical reinforcement effect was attributed mainly to good affinity and adhesion of the reinforcing agent to the biopolymeric matrix and also to the presence of stiff percolated systems of cellulose,[5,6] such as it was already hypothesized during the discussion of rheological analysis.

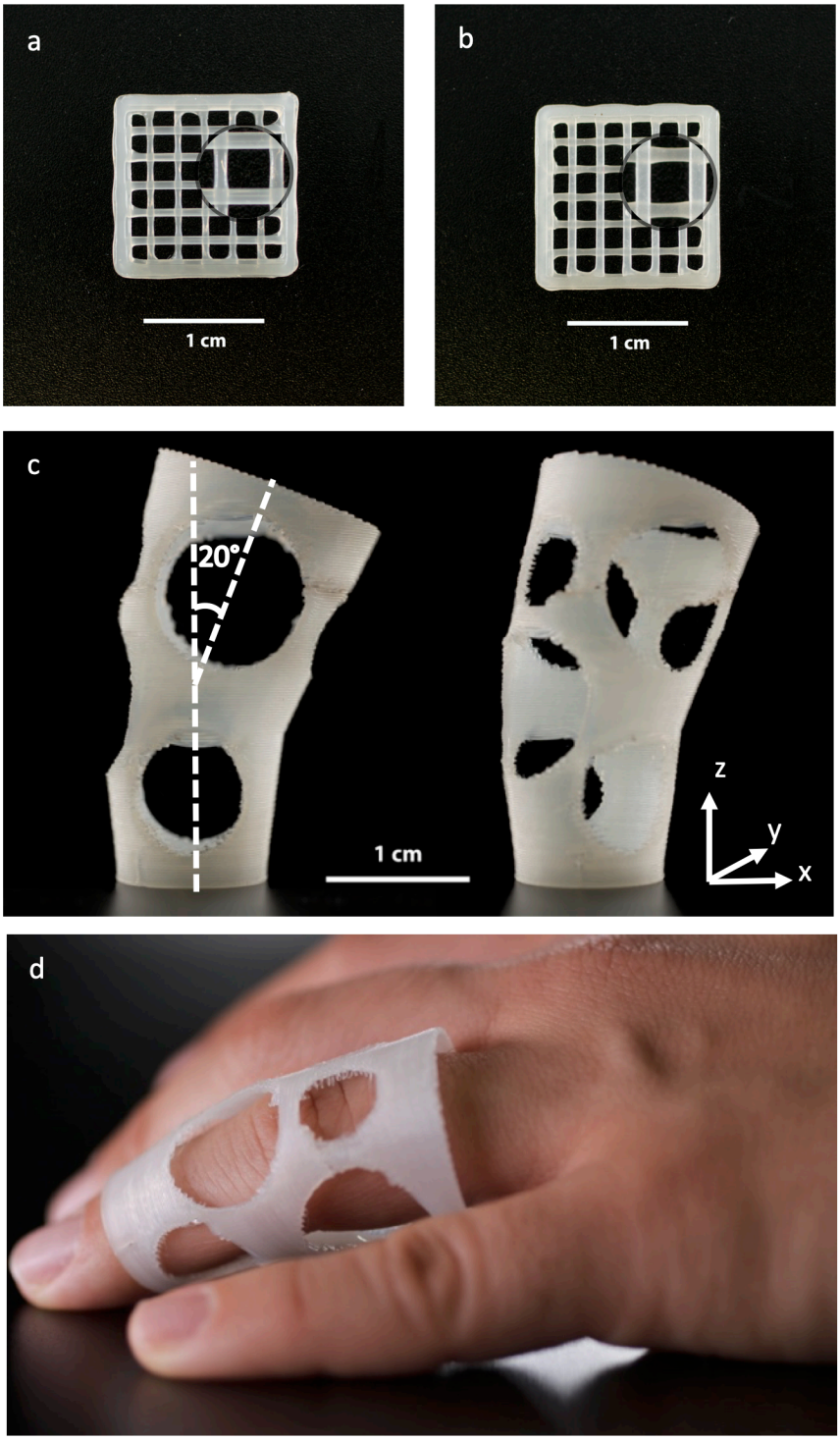

Figure 6. FDM 3D printed nanocellulose composites. Representative top view of simply shaped scaffolds printed by a filament of neat PHBH (a) and PHBH-acetylated CNC (10 wt%) composite (PHBH+CNC_AC_8_10) (b), with an alternation of 0-90° for directions of layers. Complex shaped object as a finger cast printed by a filament of PHBH composite with acetylated CNC at 10 wt% (PHBH+CNC_AC_8_10) (c). Example of use of a personalized medical device in case of finger dislocation (d).

To illustrate the printability of CNC-based composites in 3D (*x*, *y* and *z*) we FDM printed self-standing, bio-based complex-shaped objects (**Figure 6**), demonstrating the effectiveness of a solvent-free method consisting in melt compounding functionalized CNCs with PHBH matrix followed by filament preparation for the 3D printing process.

Firstly, simple 3-layer scaffolds with filling pattern alternating from 0-90° were printed with a nozzle diameter of 0.6 mm, a printing speed of 5 mm s^{-1} and an extrusion temperature of 170 °C (**Figure 6** a and b).

Both by visual and microscopy inspection, it was possible to investigate the internal porous structure, the definition of each extruded filament and pore sizes of the printed samples. They denote a good maintenance of the filamentary shape with a circular cross-section of 600 ± 15 μm, without collapsing of parts or layer delamination (see Supporting Information).

Furthermore, we printed highly complex shaped and fully customized objects, such as a wearable finger cast (**Figure 6** c and d). These medical devices were printed with similar speed and temperature of the grid-like scaffolds, but with a nozzle diameter of 0.4 mm. This wearable finger cast counts 170 layers and an inclination of the axis of 20° in the upper part, in order to best fit to the natural conformation of the finger. We highlight that the complexity of the object rises not only due to its vertical development in the *z*-direction or to the inclination of the axis (angle) but also to the close alternation of full and empty spaces and the circular shapes of the holes. This medical application could be successfully used substituting a rigid plaster in case of dislocation, resulting anyhow recyclable, custom-fitted and with the advantage that it can be taken off to wash and ventilate the injured area.

Nevertheless, not only external medical devices could be 3D printed with these innovative composites, but they could be used also in biomedical engineering, to create unique, patient-matched surgical implants for particular illnesses. Always in the biomedical field, another possible application could be the fabrications of scaffolds that could serve as biomedical templates for cell culturing or biodegradable and bioresorbable implants for tissue engineering.[53]

The possibilities of applications of these biocomposites are not only limited to the biomedical field, but it is likely to foresee a possible use also in the 3D printing of electronic devices[54] and some automotive components,[32] in order to favor the replacement of traditional petroleum-based plastic. Such an eco-friendly material could also be used to further help the environment promoting the growth of the crystalline barrier 3D printing coral-shaped structures, which encourage coral polyps to colonize and regenerate damaged reefs.[55] However, we can state that these are just some possible examples, and a much wider and auspicious range of applications, mixing the advantages of additive manufacturing with those of a bio-based and eco-friendly material with good mechanical properties and thermal stability is launched for future developments.

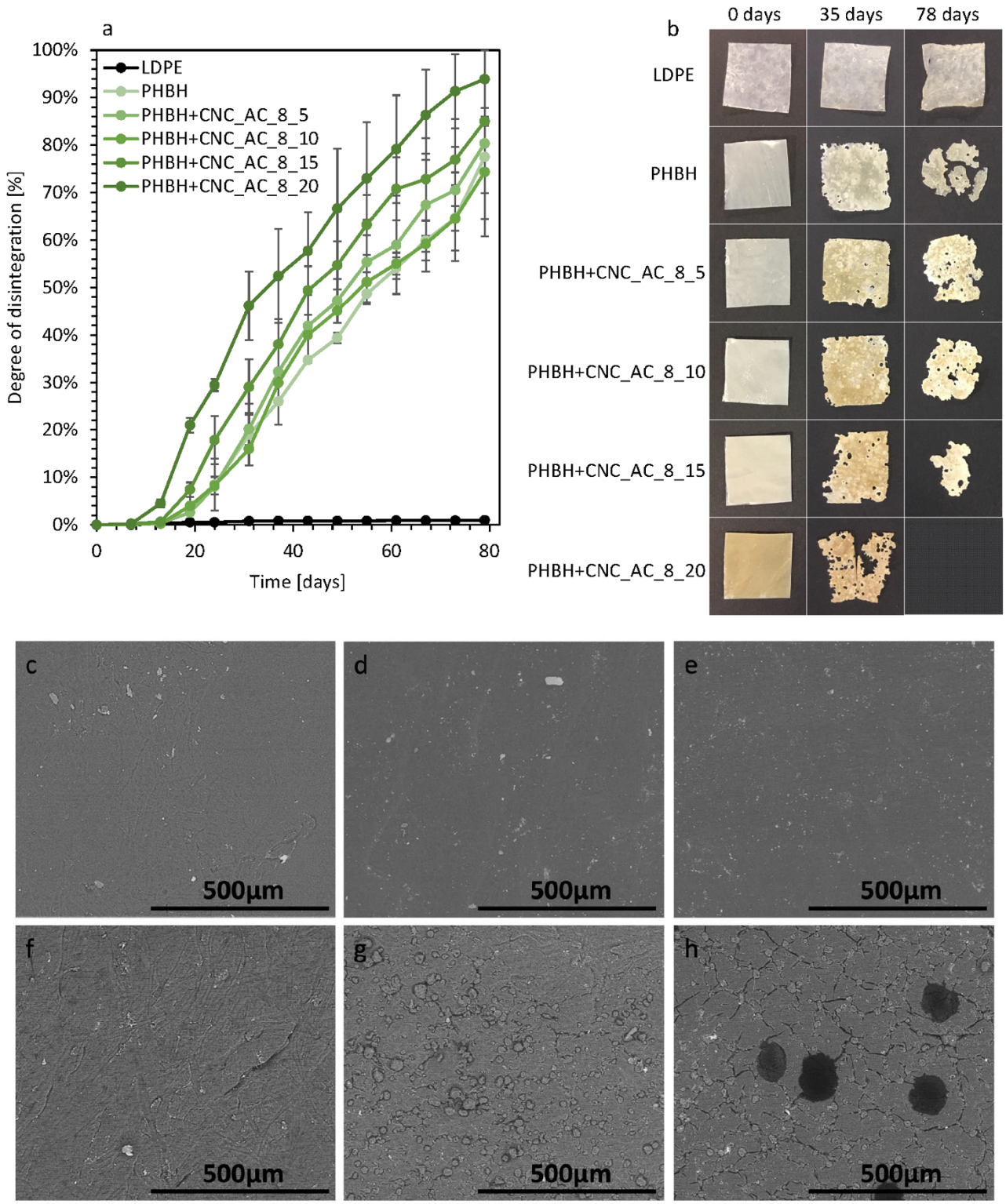

Figure 7. Disintegration of the PHBH bio-composites and of a traditional petroleum-based low-density polyethylene over time and under composting conditions in a laboratory-scale test. Plot of the degree of disintegration as a function of the time and CNC content (a). Visual appearance of the tested composites films (PHBH+CNC_AC) at starting moment, after 35 days and 78 days during the composting process (b). ESEM micrographs of the LDPE samples at different degradation times: starting moment (c), after 35 days (d) and 78 days (e). ESEM micrographs of the CNC_AC_8_15 samples, chosen as representative for the behavior of the bio-based composites, at different degradation times: starting moment (f), after 35 days (g) and 78 days (h).

Biodegradability tests were conducted to study the degree of disintegration of the composites in composting conditions (**Figure 7**). To this end, we evaluated the weight loss of pristine biopolymer PHBH, the CNC-reinforced PHBH composites and compared it with petroleum-based low-density polyethylene

(LDPE). The tests were performed according to the ISO 20200 standard. The comparison of the obtained results allows us to appreciate the actual biodegradation of these innovative composites, compared to a traditional thermoplastic polymer.

Degree of disintegration of the neat polymers and composites was plotted as a function of time and composition (**Figure 7**a). As expected, LDPE was not morphologically affected by the composting conditions, showing almost perfect mass conservation even after 78 days (**Figure 7**b). On the contrary, neat PHBH and PHBH+CNC_AC_8 composites denote an evident trend of an increased degree of disintegration over the composting time. In the first two weeks, the weight loss remained practically unchanged, as it has already been noted previously,[56] since in this first step of biodegradation, only small molecules can be degraded, and this is indicated by a roughening of the surface. In fact, polyhydroxyalkanoate disintegration is primarily caused by microorganisms that erode the polymer surface and gradually spread into the bulk.[56,57] After 15 days, the maturation stage started and a rapid increase in the degree of disintegration is observed, with no tendency to a plateau. This second stage is characterized by the biodegradation of high-molecular weight materials such as PHBH, CNC, and biomass present in the compost.[56]

Within the first three months of the composting process, all bio-based samples reached a degree of disintegration higher than 75 %. Weight loss rate increased with the increase of acetylated CNC content; in fact, the highest degree of disintegration was measured for PHBH+CNC_AC_8_20, with a weight loss of 94 % after 78 days. Hence, it seems that cellulose nanocrystals affect also the disintegration process of the biopolymer, thereby increasing the biodegradability of the composites, according to the CNCs content. Puglia *et al.* observed that montmorillonite favors the presence of residual water and the hydrolysis of polymer chains into smaller molecules digestible by microorganisms.[57] Similarly, the same hypothesis might be extended also for CNC.

The morphological changes of the samples were investigated at different composting times; firstly, by visual appearance to assess the macroscopic impact of degradation over time (**Figure 7** b); and secondly, by ESEM observation (**Figure 7** c to h). The goal was to show the heterogeneity and roughness of the surface of the bio-based and biodegradable samples, characterized by the presence of holes, cavities and cracks. On the other hand, LDPE did not denote a significant alteration of the mass nor of the surface morphology; and this supports the great difference existing between the sustainable end-of-life of the bio-based PHBH-nanocellulose composites over a traditional petroleum-based plastic such as LDPE, which is completely resistant to a composting process even for long periods.

CONCLUSIONS

We have demonstrated a successful method for 3D printing CNC-reinforced biopolymer composites by FDM. The followed functionalization is a solvent-free process, which enhanced the affinity between the biodegradable PHBH matrix and the cellulose nanocrystals. The compounding procedure adopted here is also free of any toxic solvent as we did it via a melt-compounding approach that enabled high reinforcing content from 5 wt% up to 20 wt% of acetylated CNC. Our method allows for considerable improvement of thermal and thermo-mechanical properties of neat PHBH. CNC reinforcement effects cause a shift towards higher thermal stability temperatures, which vary from 220 °C for neat PHBH to 265 °C for composites. Storage modulus has shown 150 % increase in values for 20 wt% CNC_AC_8 composites. Furthermore, the findings of this research show that CNC, in addition to enhancing the thermal and mechanical properties of the bio-composites, also offers a way to tune the degree of disintegration of the composite materials, in line with the nanocellulose content. From this material, constant size filaments were experimentally obtained and used for 3D FDM printing. The prepared bio-based filaments were employed to successfully print different architectures, also with complex and extended shapes. The disintegration test showed an expected difference between a traditional thermoplastic, with no degradation during the composting process, and the PHBH+CNC_AC_8 biocomposites, whose degree of disintegration increased with respect to the acetylated CNC content, up to a maximum weight loss of 94 % after 78 days.

This promising material and this adaptable approach open great opportunities for the development of novel grade of printable customized materials with tunable mechanical properties and different possible applications for bio-based, sustainable and biodegradable designs, with improved properties. This work combines positively the advantages of eco-friendly materials such as PHBH and CNC with the advantages of additive manufacturing and its tailoring properties.

ASSOCIATED CONTENT

Supporting Information

The Supporting Information is available free of charge on the ACS Publications website.

Rheological behavior, thermal stability and dynamic mechanical analysis of compounded materials with different acetylated CNC content and pristine PHBH; optical microscopy of 3D printed objects by fused deposition modeling (PDF)

ACKNOWLEDGMENT

The authors thank Anja Huch for the TEM imaging, Electra Maria Letizia D'Emilio for the photographs of 3D printed samples. The authors are also thankful to Dr. Tutu Sebastian for TGA measurements and for the support while using specific equipment. The authors thank as well MAIP Group (MAIP SRL, Turin, Italy) for supplying the PHBH pellets.

REFERENCES

(1) Ouyang, S. P.; Liu, Q.; Fang, L.; Chen, G. Q. Construction of Pha-Operon-Defined Knockout Mutants of Pseudomonas Putida KT2442 and Their Applications in Poly(Hydroxyalkanoate) Production. Macromol. Biosci. 2007, 7 (2), 227–233. https://doi.org/10.1002/mabi.200600187.

(2) Hosoda, N.; Tsujimoto, T.; Uyama, H. Green Composite of Poly(3-Hydroxybutyrate-Co-3-Hydroxyhexanoate) Reinforced with Porous Cellulose. ACS Sustain. Chem. Eng. 2014, 2 (2), 248–253. https://doi.org/10.1021/sc400290y.

(3) Willson, A.; Takashi, K. Effects of Glass Fibers on Mechanical and Thermal Properties of Poly(3-Hydroxybutyrate-Co-3-Hydroxyhexanoate). Polym. Compos. 2018, 39, 491–503.

(4) Mahmood, H.; Pegoretti, A.; Brusa, R. S.; Ceccato, R.; Penasa, L.; Tarter, S.; Checchetto, R. Molecular Transport through 3-Hydroxybutyrate Co-3-Hydroxyhexanoate Biopolymer Films with Dispersed Graphene Oxide Nanoparticles: Gas Barrier, Structural and Mechanical Properties. Polym. Test. 2020, 81 (July 2019), 106181. https://doi.org/10.1016/j.polymertesting.2019.106181.

(5) Zhou, J.; Ma, X.; Li, J.; Zhu, L. Preparation and Characterization of a Bionanocomposite from Poly (3-Hydroxybutyrate-Co-3-Hydroxyhexanoate) and Cellulose Nanocrystals. Cellulose 2019, 26 (2), 979–990. https://doi.org/10.1007/s10570-018-2136-1.

(6) Li, D.; Zhou, J.; Ma, X.; Li, J. Synthesis of a Novel Biocomposite of Poly (3-Hydroxybutyrate-Co-3-Hydroxyhexanoate) Reinforced with Acetylated Cellulose Nanocrystals. Cellulose 2019, 26 (16), 8729–8743. https://doi.org/10.1007/s10570-019-02708-2.

(7) Mondal, S. Preparation, Properties and Applications of Nanocellulosic Materials. Carbohydr. Polym. 2017, 163, 301–316. https://doi.org/10.1016/j.carbpol.2016.12.050.

(8) Mishra, R. K.; Sabu, A.; Tiwari, S. K. Materials Chemistry and the Futurist Eco-Friendly Applications of Nanocellulose: Status and Prospect. J. Saudi Chem. Soc. 2018, 22 (8), 949–978. https://doi.org/10.1016/j.jscs.2018.02.005.

(9) Giubilini, A.; Sciancalepore, C.; Messori, M.; Bondioli, F. New Biocomposite Obtained Using Poly(3-Hydroxybutyrate-Co-3-Hydroxyhexanoate) (PHBH) and Microfibrillated Cellulose. J. Appl. Polym. Sci. 2020, 48953, 6–13. https://doi.org/10.1002/app.48953.

(10) Mahfoudhi, N.; Boufi, S. Nanocellulose as a Millennium Material with Enhancing Adsorption Capacities. In Biodegradable and Biobased Polymers for Environmental and Biomedical Applications; 2016; pp 349–383. https://doi.org/10.1002/9781119117360.ch10.

(11) Wu, X.; Moon, R. J.; Martini, A. Crystalline Cellulose Elastic Modulus Predicted by Atomistic Models of Uniform Deformation and Nanoscale Indentation. Cellulose 2013, 20 (1), 43–55. https://doi.org/10.1007/s10570-012-9823-0.

(12) Dufresne, A. 5. Chemical Modification of Nanocellulose. In Nanocellulose: From Nature to High Performance Tailored Materials; 2017; pp 221–286. https://doi.org/10.1515/9783110480412-006.

(13) Espino-Pérez, E.; Bras, J.; Ducruet, V.; Guinault, A.; Dufresne, A.; Domenek, S. Influence of Chemical Surface Modification of Cellulose Nanowhiskers on Thermal, Mechanical, and Barrier Properties of Poly(Lactide) Based Bionanocomposites. Eur. Polym. J. 2013, 49 (10), 3144–3154. https://doi.org/10.1016/j.eurpolymj.2013.07.017.

(14) Yano, H.; Omura, H.; Honma, Y.; Okumura, H.; Sano, H.; Nakatsubo, F. Designing Cellulose Nanofiber Surface for High Density Polyethylene Reinforcement. Cellulose 2018, 25 (6), 3351–3362. https://doi.org/10.1007/s10570-018-1787-2.

(15) Wang, Y.; Wang, X.; Xie, Y.; Zhang, K. Functional Nanomaterials through Esterification of Cellulose: A Review of Chemistry and Application. Cellulose 2018, 25 (7), 3703–3731. https://doi.org/10.1007/s10570-018-1830-3.

(16) Zimmermann, M. V. G.; da Silva, M. P.; Zattera, A. J.; Campomanes Santana, R. M. Effect of Nanocellulose Fibers and Acetylated Nanocellulose Fibers on Properties of Poly(Ethylene-Co-Vinyl Acetate) Foams. J. Appl. Polym. Sci. 2017, 134 (17), 1–12. https://doi.org/10.1002/app.44760.

(17) Barbosa, R. F. S.; Souza, A. G.; Ferreira, F. F.; Rosa, D. S. Isolation and Acetylation of Cellulose Nanostructures with a Homogeneous System. Carbohydr. Polym. 2019, 218 (February), 208–217. https://doi.org/10.1016/j.carbpol.2019.04.072.

(18) Frank, B. P.; Durkin, D. P.; Caudill, E. R.; Zhu, L.; White, D. H.; Curry, M. L.; Pedersen, J. A.; Fairbrother, D. H. Impact of Silanization on the Structure, Dispersion Properties, and Biodegradability of Nanocellulose as a Nanocomposite Filler. ACS Appl. Nano Mater. 2018, 1 (12), 7025–7038. https://doi.org/10.1021/acsanm.8b01819.

(19) Beaumont, M.; Bacher, M.; Opietnik, M.; Gindl-Altmutter, W.; Potthast, A.; Rosenau, T. A General Aqueous Silanization Protocol to Introduce Vinyl, Mercapto or Azido Functionalities onto Cellulose Fibers and Nanocelluloses. Molecules 2018, 23 (6), 1–15. https://doi.org/10.3390/molecules23061427.

(20) Fujisawa, S.; Ikeuchi, T.; Takeuchi, M.; Saito, T.; Isogai, A. Superior Reinforcement Effect of TEMPO-Oxidized Cellulose Nanofibrils in Polystyrene Matrix: Optical, Thermal, and Mechanical Studies. Biomacromolecules 2012, 13 (7), 2188–2194. https://doi.org/10.1021/bm300609c.

(21) Carlsson, D. O.; Lindh, J.; Nyholm, L.; Strømme, M.; Mihranyan, A. Cooxidant-Free TEMPO-Mediated Oxidation of Highly Crystalline Nanocellulose in Water. RSC Adv. 2014, 4 (94), 52289–52298. https://doi.org/10.1039/c4ra11182f.

(22) Tan, C.; Peng, J.; Lin, W.; Xing, Y.; Xu, K.; Wu, J.; Chen, M. Role of Surface Modification and Mechanical Orientation on Property Enhancement of Cellulose Nanocrystals/Polymer Nanocomposites. Eur. Polym. J. 2015, 62, 186–197. https://doi.org/10.1016/j.eurpolymj.2014.11.033.

(23) Wei, L.; McDonald, A. G.; Stark, N. M. Grafting of Bacterial Polyhydroxybutyrate (PHB) onto Cellulose via In Situ Reactive Extrusion with Dicumyl Peroxide. Biomacromolecules 2015, 16 (3), 1040–1049. https://doi.org/10.1021/acs.biomac.5b00049.

(24) Barsbay, M.; Güven, O. Surface Modification of Cellulose via Conventional and Controlled Radiation-Induced Grafting. Radiation Physics and Chemistry. Elsevier Ltd July 1, 2019, pp 1–8. https://doi.org/10.1016/j.radphyschem.2019.03.002.

(25) Oksman, K.; Aitomäki, Y.; Mathew, A. P.; Siqueira, G.; Zhou, Q.; Butylina, S.; Tanpichai, S.; Zhou, X.; Hooshmand, S. Review of the Recent Developments in Cellulose Nanocomposite Processing. Compos. Part A Appl. Sci. Manuf. 2016, 83, 2–18. https://doi.org/10.1016/j.compositesa.2015.10.041.

(26) Dufresne, A. Cellulose Nanomaterials as Green Nanoreinforcements for Polymer Nanocomposites. Philos. Trans. R. Soc. 2017, 376, 1–23.

(27) Gan, P. G.; Sam, S. T.; Abdullah, M. F. bin; Omar, M. F. Thermal Properties of Nanocellulose-reinforced Composites: A Review. J. Appl. Polym. Sci. 2020, 137 (11), 48544. https://doi.org/10.1002/app.48544.

(28) Xu, X.; Li, J.; Ma, L.; Ma, X. Preparation and Properties of Biocomposite from Poly(3-Hydroxybutyrate-Co-3-Hydroxyhexanoate) Reinforced with Regenerated Cellulose. Cellulose 2019, 26 (9), 5427–5436. https://doi.org/10.1007/s10570-019-02460-7.

(29) Rahim, T. N. A. T.; Abdullah, A. M.; Md Akil, H. Recent Developments in Fused Deposition Modeling-Based 3D Printing of

Polymers and Their Composites. Polym. Rev. 2019, 59 (4), 589–624. https://doi.org/10.1080/15583724.2019.1597883.

(30) Vyavahare, S.; Teraiya, S.; Panghal, D.; Kumar, S. Fused Deposition Modelling: A Review. Rapid Prototyp. J. 2020, 26 (1), 176–201. https://doi.org/10.1108/RPJ-04-2019-0106.

(31) Dilberoglu, U. M.; Simsek, S.; Yaman, U. Shrinkage Compensation Approach Proposed for ABS Material in FDM Process. Mater. Manuf. Process. 2019, 34 (9), 993–998. https://doi.org/10.1080/10426914.2019.1594252.

(32) Schmitt, M.; Mehta, R. M.; Kim, I. Y. Additive Manufacturing Infill Optimization for Automotive 3D-Printed ABS Components. Rapid Prototyp. J. 2020, 26 (1), 89–99. https://doi.org/10.1108/RPJ-01-2019-0007.

(33) Wu, D.; Spanou, A.; Diez-Escudero, A.; Persson, C. 3D-Printed PLA/HA Composite Structures as Synthetic Trabecular Bone: A Feasibility Study Using Fused Deposition Modeling. J. Mech. Behav. Biomed. Mater. 2020, 103 (August 2019), 103608. https://doi.org/10.1016/j.jmbbm.2019.103608.

(34) Dave, H. K.; Prajapati, A. R.; Rajpurohit, S. R.; Patadiya, N. H.; Raval, H. K. Open Hole Tensile Testing of 3D Printed Parts Using In-House Fabricated PLA Filament. Rapid Prototyp. J. 2020, 26 (1), 21–31. https://doi.org/10.1108/RPJ-01-2019-0003.

(35) Prasad, A.; Kandasubramanian, B. Fused Deposition Processing Polycaprolactone of Composites for Biomedical Applications. Polym. Technol. Mater. 2019, 58 (13), 1365–1398. https://doi.org/10.1080/25740881.2018.1563117.

(36) Hedayati, S. K.; Behravesh, A. H.; Hasannia, S.; Bagheri Saed, A.; Akhoundi, B. 3D Printed PCL Scaffold Reinforced with Continuous Biodegradable Fiber Yarn: A Study on Mechanical and Cell Viability Properties. Polym. Test. 2020, 83 (January), 106347. https://doi.org/10.1016/j.polymertesting.2020.106347.

(37) Valentini, F.; Dorigato, A.; Rigotti, D.; Pegoretti, A. Polyhydroxyalkanoates/Fibrillated Nanocellulose Composites for Additive Manufacturing. J. Polym. Environ. 2019, 27, 1333–1341. https://doi.org/10.1007/s10924-019-01429-8.

(38) Olaru, N.; Olaru, L.; Vasile, C.; Ander, P. Surface Modified Cellulose Obtained by Acetylation without Solvents of Bleached and Unbleached Kraft Pulps. Polimery 2011, 56 (11/12), 834–840. https://doi.org/10.14314/polimery.2011.834.

(39) Ou-Yang, Q.; Guo, B.; Xu, J. Preparation and Characterization of Poly(Butylene Succinate)/Polylactide Blends for Fused Deposition Modeling 3D Printing. ACS Omega 2018, 3 (10), 14309–14317. https://doi.org/10.1021/acsomega.8b02549.

(40) Tingaut, P.; Zimmermann, T.; Lopez-Suevos, F. Synthesis and Characterization of Bionanocomposites with Tunable Properties from Poly(Lactic Acid) and Acetylated Microfibrillated Cellulose. Biomacromolecules 2010, 11 (2), 454–464. https://doi.org/10.1021/bm901186u.

(41) Li, W.; Cai, G.; Zhang, P. A Simple and Rapid Fourier Transform Infrared Method for the Determination of the Degree of Acetyl Substitution of Cellulose Nanocrystals. J. Mater. Sci. 2019, 54 (10), 8047–8056. https://doi.org/10.1007/s10853-019-03471-2.

(42) Xu, C.; Chen, J.; Wu, D.; Chen, Y.; Lv, Q.; Wang, M. Polylactide/Acetylated Nanocrystalline Cellulose Composites Prepared by a Continuous Route: A Phase Interface-Property Relation Study. Carbohydr. Polym. 2016, 146, 58–66. https://doi.org/10.1016/j.carbpol.2016.03.058.

(43) Lin, N.; Huang, J.; Chang, P. R.; Feng, J.; Yu, J. Surface Acetylation of Cellulose Nanocrystal and Its Reinforcing Function in Poly(Lactic Acid). Carbohydr. Polym. 2011, 83 (4), 1834–1842. https://doi.org/10.1016/j.carbpol.2010.10.047.

(44) Popescu, C. M.; Larsson, P. T.; Olaru, N.; Vasile, C. Spectroscopic Study of Acetylated Kraft Pulp Fibers. Carbohydr. Polym. 2012, 88 (2), 530–536. https://doi.org/10.1016/j.carbpol.2011.12.046.

(45) Huang, K.; Zhang, M.; Zhang, G.; Jiang, X.; Huang, D. Acetylation Modification of Rice Straw Fiber and Its Thermal Properties. Cellul. Chem. Technol. 2014, 48 (3–4), 199–207.

(46) Carreau, P. J. Rheological Equations from Molecular Network Theories. J. Rheol. (N. Y. N. Y). 1972, 16 (1), 99–127.

(47) Ching, Y. C.; Ershad Ali, M.; Abdullah, L. C.; Choo, K. W.; Kuan, Y. C.; Julaihi, S. J.; Chuah, C. H.; Liou, N. S. Rheological Properties of Cellulose Nanocrystal-Embedded Polymer Composites: A Review. Cellulose 2016, 23 (2), 1011–1030. https://doi.org/10.1007/s10570-016-0868-3.

(48) Esposito Corcione, C.; Scalera, F.; Gervaso, F.; Montagna, F.; Sannino, A.; Maffezzoli, A. One-Step Solvent-Free Process for the Fabrication of High Loaded PLA/HA Composite Filament for 3D Printing. J. Therm. Anal. Calorim. 2018, 134 (1), 575–582. https://doi.org/10.1007/s10973-018-7155-5.

(49) Qahtani, M.; Wu, F.; Misra, M.; Gregori, S.; Mielewski, D. F.; Mohanty, A. K. Experimental Design of Sustainable 3D-Printed Poly(Lactic Acid)/Biobased Poly(Butylene Succinate) Blends via Fused Deposition Modeling. ACS Sustain. Chem. Eng. 2019, 7 (17), 14460–14470. https://doi.org/10.1021/acssuschemeng.9b01830.

(50) Li, S.; He, J.; Yu, P. H.; Cheung, M. K. Thermal Degradation of Poly (3-Hydroxybutyrate) and Poly (3-Hydroxybutyrate- Co -3-Hydroxyvalerate) as Studied by TG , TG – FTIR , and Py – GC / MS. J. Appl. Polym. Sci. 2003, 89, 1530–1536.

(51) Erceg, M.; Kovačić, T.; Klarić, I. Dynamic Thermogravimetric Degradation of Poly(3-Hydroxybutyrate)/Aliphatic- Aromatic Copolyester Blends. Polym. Degrad. Stab. 2005, 90 (1), 86–94. https://doi.org/10.1016/j.polymdegradstab.2005.02.014.

(52) Yu, H. Y.; Qin, Z. Y.; Liu, Y. N.; Chen, L.; Liu, N.; Zhou, Z. Simultaneous Improvement of Mechanical Properties and Thermal Stability of Bacterial Polyester by Cellulose Nanocrystals. Carbohydr. Polym. 2012, 89 (3), 971–978. https://doi.org/10.1016/j.carbpol.2012.04.053.

(53) Koller, M. Biodegradable and Biocompatible Polyhydroxy-Alkanoates (PHA): Auspicious Microbial Macromolecules for Pharmaceutical and Therapeutic Applications. Molecules 2018, 23 (362), 1–20. https://doi.org/10.3390/molecules23020362.

(54) Guo, R.; Ren, Z.; Bi, H.; Xu, M.; Cai, L. Electrical and Thermal Conductivity of Polylactic Acid (PLA)-Based Biocomposites by Incorporation of Nano-Graphite Fabricated with Fused Deposition Modeling. Polymers (Basel). 2019, 11 (549), 1–19. https://doi.org/10.3390/polym11030549.

(55) Ruhl, E. J.; Dixson, D. L. 3D Printed Objects Do Not Impact the Behavior of a Coral-Associated Damselfish or Survival of a Settling Stony Coral. PLoS One 2019, 14 (8), 1–12. https://doi.org/10.1371/journal.pone.0221157.

(56) Iggui, K.; Le Moigne, N.; Kaci, M.; Cambe, S.; Degorce-Dumas, J. R.; Bergeret, A. A Biodegradation Study of Poly(3-Hydroxybutyrate-Co-3-Hydroxyvalerate)/Organoclay Nanocomposites in Various Environmental Conditions. Polym. Degrad. Stab. 2015, 119, 77–86. https://doi.org/10.1016/j.polymdegradstab.2015.05.002.

(57) Puglia, D.; Fortunati, E.; D'Amico, D. A.; Manfredi, L. B.; Cyras, V. P.; Kenny, J. M. Influence of Organically Modified Clays on the Properties and Disintegrability in Compost of Solution Cast Poly(3-Hydroxybutyrate) Films. Polym. Degrad. Stab. 2014, 99 (1), 127–135. https://doi.org/10.1016/j.polymdegradstab.2013.11.013.

Table of Contents artwork

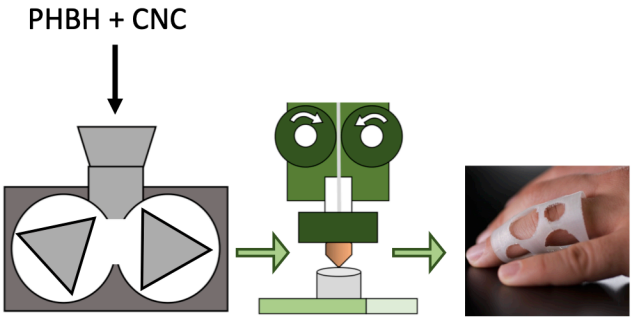

Synopsis:

A fully bio-based and biodegradable composite material was fabricated for 3D printing complex architectures for different application fields (i.e. medical, electrical, automotive..), combining the advantages of eco-friendly materials with the advantages of additive manufacturing and its tailoring properties.